

Aggregation properties of carbon nanotubes at interfaces

Ross Tucknott, S.N. Yaliraki*

Department of Chemistry, Imperial College of Science, Technology and Medicine, Exhibition Road, London SW7 2AY, UK

Received 1 March 2002

Abstract

Single-walled carbon nanotubes (SWNTs) are emerging as promising candidates for molecular electronic device components. However, to obtain individual SWNTs and to place them controllably at interfaces remains a major hurdle. This is crucial because transport depends dramatically and subtly on the relative orientation of wires. We study theoretically the aggregation of dispersed individual SWNTs on a surface. We pay particular attention to the anisotropic orientational dependence of the van der Waals (vdW) interaction between tubes as well as that of the tube with the surface. We find that at experimentally relevant regimes, tubes form clusters of different sizes that depend on the density. Even for very low densities, individual tubes are improbable. © 2002 Elsevier Science B.V. All rights reserved.

1. Introduction

A series of advances in such diverse disciplines as supramolecular chemistry [1] and single molecule techniques [2] has led to remarkable experimental demonstrations of molecules functioning as components of conventional electrical circuitry: wires [3,4], reconfigurable switches [5], amplifiers [6], field-effect transistors [7], memories [8]. During the past year, not only components but logic circuits have also been reported [9–12]. However, for the promise of individual molecules or molecular monolayers to function as electronic devices [13] the problem of their chemical assembly in controllable, scalable and efficient arrangements needs to be overcome.

These difficulties are exemplified by the case of single-walled carbon nanotubes (SWNTs). Since their discovery [14], their remarkable electronic as well as mechanical properties [15] have made them ideal candidates for elements in molecular devices. However, they remain notoriously difficult to solubilise or otherwise manipulate chemically. To date, efforts to organize them have relied on fortuitous events such as spattering, or alternatively, on techniques involving extensive lithography, such as fluidics [16], surface patterning [17] or direct growth out of an electrode [18]. Two experimental routes that depend instead on molecular properties have been proposed: electric field manipulation [19,20] and polymer-wrapping [21,22]. Both methods aim at first to overcome the same obstacle, namely, the bundling or roping of tubes that results from their strong van der Waals (vdW) attractions.

Carbon nanotubes have a strong tendency to orient parallel to each other due to the strong vdW

* Corresponding author. Fax: +44-207-594-5880.
E-mail address: s.yaliraki@ic.ac.uk (S.N. Yaliraki).

forces: the tubes arrange themselves in a hexagonal structure within the ropes [23], with a binding energy of several hundreds of meV/nm [24]. Throughout the paper, we refer to the hexagonal packing of parallel tubes as *rope* or *bundle*, and to other arrangements as *aggregates*. Breaking up these bundles to obtain individual tubes of uniform size and type continues to be a central unsolved experimental problem. Even with a technique such as sonication, that partially dismantles bundles and produces individual tubes, little is known about the subsequent solubility of carbon nanotubes and their organisation in structures other than ropes. Yet, proposed molecular devices frequently rely on such an organisation [25]. In particular, the fabrication of a crossbar (an array or square lattice made of nanotubes on a surface) is currently a subject of intense research [16,20]. The quest for such an array is motivated by a default-tolerant molecular-based computer proposed in 1998 [25].

Given the need to achieve such controlled aggregation of nanotubes, it is surprising that it has been little explored theoretically in the literature. The formation of ropes and their ensuing properties have been intensely studied, but work so far has concentrated either on properties of single nanotubes or on properties of perfectly formed ropes [26–28]. Here, we are concerned with the opposite problem: namely, how to keep individual nanotubes from forming ropes and how alternative structures may be formed. Furthermore, the role of an interface in the aggregation process needs to be addressed since in a device the tubes are usually in contact with an electrode.

Additionally, it is important to study structure because it is ultimately correlated with function. It has been shown, both experimentally [29,30] and theoretically, that the conductance depends strongly on the geometry [31–33], the conformation, and the number [34–36] of molecules involved (see however, [37]). So far, charge transport on a crossed nanotube junction exhibits rich behaviour not well understood [11,38]. Unraveling the microscopic interactions that lead to the architectures of the self-assembling molecular structures at the interface is a first step for controlling transport.

The purpose of this paper is to address this issue. First, we study the aggregation properties of model SWNTs on a surface as a result of the competition of the highly anisotropic attractive vdW interactions aligning the tubes and their interaction with the surface. Understanding how the tubes aggregate opens the way to producing individual nanotubes. In particular, we investigate on one extreme, the possibility of tubes remaining isolated, and on the other, the formation of arrays, rather than ropes.

2. Model

We consider individual SWNTs dispersed on a surface after sonication or an equivalent technique. Only tubes that make contact with the surface are considered that is, we ignore the reservoir of tubes in the solution. Tubes are free to move on the surface or take different orientations, but do not detach themselves. We model the tubes as one-dimensional hollow rods of length L , with a uniform density of carbon atoms per unit length. We choose a (10,10) equivalent structure due to its predominance in the literature over most others. We focus on short tubes (10 nm long, 1.3 nm wide) since sonication not only breaks ropes but also cuts SWNTs. These tubes exhibit negligible radial compression whilst on a surface [39], making the assumption of a rigid rod model to be valid with respect to the tube–surface interaction. We ignore the elastic deformation that tubes may experience as they come into contact with the substrate or other tubes. This is estimated to give an error of less than 2% for SWNTs of the size we are considering but may be considerably more important for bigger or multi-walled tubes [39]. In this work we have considered a graphite surface whose interaction with the tubes is fairly well known. We take into account all the interactions as tubes take different orientations. We consider the attractive and repulsive interactions between nanotube pairs and each individual nanotube and the surface. It is the van der Waals (vdW) interactions that govern the aggregation behaviour in these systems. Here, we restrict the discussion to the effective pair potential; that is, we disregard interactions of three

and higher order body forces. We take the cut-off for interaction at 20 nm, substantially longer than nearest-neighbours. In general this interaction is very complex and still not fully understood for attractive rods [40,41]. Our potential consists of two parts,

$$V_{\text{total}} = V_{\text{tt}} + V_{\text{ts}}, \quad (1)$$

where V_{tt} corresponds to tube–tube interactions and V_{ts} describes the interaction of each individual tube with the surface. We describe the potential in some detail in the following section.

2.1. Potential of tube–tube and tube–surface interaction

The vdW attraction and the crossover to repulsion at small separation is adequately described by a Lennard-Jones potential:

$$V_{\text{LJ}} = -A/R^6 + B/R^{12} \quad (2)$$

after pairwise summation of the microscopic interactions.

Girifalco has integrated the above potential for carbon–carbon atoms over two spherical shells, to obtain the effective potential between two C_{60} s [42], and between two infinite parallel hollow cylinders, to approximate the interaction between two carbon nanotubes parallel to each other [24]. These potentials have been successful in describing several material properties of nanotube crystals. However, only parallel, infinitely long tubes have been considered. The purpose of this work is to examine the structural properties of short tubes, in non-parallel orientations in the presence of a surface.

To go from Eq. (2) to the continuum, the density of atoms must be known. Alternatively, a discrete approach may be taken, where each atom is assumed to be at the centre of a symmetric electron distribution. Despite the different merits of the continuum vs. the discrete approach, they seem to give similar results when the same parameters are chosen [24]. Here, we use the continuum approach with numerical integration. The atomic density per unit length of the tube was calculated from the geometry of the tubes. Each tube is represented as a collection of segments. The

tubes can take a discrete number of orientations. One end of each tube was constrained to remain fixed to lattice points on the plane of the surface, defined as the x – y plane of the system. The position of the tube is then characterised by four parameters (see Fig. 1): two co-ordinates x and y (constrained by the dimensions of the lattice) and the two angles θ (angle between the tube and the surface, measured perpendicular to the x – y plane, between 0° – 90° in 10° intervals) and ϕ (angle between the tube and the y -axis, between 5 – 355° in 10° intervals).

The potential was calculated by measuring the distance between the centres of two tube segments of the same length, and hence the same number of constituent atoms; obtaining the potential energy between the two segments V_{segment} , and summing up the contributions from all the segments of one tube with all the segments of the other:

$$V_{\text{tt}} = \frac{1}{2} \sum_{m=1}^{\#\text{sgmts}} \sum_{n=1}^{\#\text{sgmts}} V_{\text{segment}}(R(n, m)).$$

We found that 100 segments for each tube were enough to reproduce accurately the results of

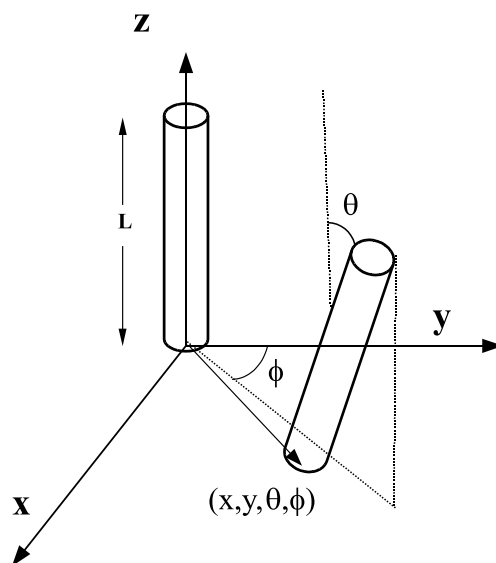


Fig. 1. The configuration of two tubes represented by rods of length L , on a surface in the x, y plane. Each tube is represented by four points, the x and y coordinates and the angles θ and ϕ . The interaction potential V_{total} is described in detail in the text using this convention.

numerical integration. The inter-segment potential relied on the Lennard–Jones potential

$$V_{\text{segment}}(R) = -C_6A/R^6 + C_{12}B/R^{12}, \quad (3)$$

where C_6 and C_{12} are the standard Lennard–Jones parameters for two carbon atoms, R is the inter-segmental distance, and A and B are constants dependent upon the degree of tube discretisation and the atomic density.

Expanding each Cartesian coordinate of the distance R ,

$$\begin{aligned} \Delta x(n, m) &= (x_1 - n dx_1) - (x_2 - m dx_2) \\ &= x_0 - K_2(n \sin \theta_1 \sin \phi_1 - m \sin \theta_2 \sin \phi_2), \end{aligned}$$

$$\begin{aligned} \Delta y(n, m) &= (y_1 - n dy_1) - (y_2 - m dy_2) \\ &= y_0 - K_2(n \sin \theta_1 \cos \phi_1 - m \sin \theta_2 \cos \phi_2), \end{aligned}$$

$$\begin{aligned} \Delta z(n, m) &= (z_1 - n dz_1) - (z_2 - m dz_2) \\ &= z_0 - K_2(n \cos \theta_1 - m \cos \theta_2), \end{aligned}$$

where $x_0 = x_1 - x_2$, etc., K_2 is a segmentation constant, n and m denote the particular segments on each tube, and dx_1 , etc., is the difference in coordinate x between subsequent segments, leads to

$$\begin{aligned} R(n, m)^2 &= K_1 - 2K_2(n \sin \theta_1(x_0 \sin \phi_1 + y_0 \cos \phi_1) \\ &\quad - m \sin \theta_2(x_0 \sin \phi_2 + y_0 \cos \phi_2) \\ &\quad + K_2(n^2 + m^2) - 2K_2^2 nm \\ &\quad \times (\sin \theta_1 \sin \theta_2 (\cos(\phi_1 - \phi_2) \\ &\quad + \cos \theta_1 \cos \theta_2)). \end{aligned} \quad (4)$$

The trigonometric values relate to the orientational parameters of the tubes, and are thus constant for a given inter-tube potential calculation. K_1 is given by $K_1 = x_0^2 + y_0^2 + z_0^2$.

This simple treatment is enhanced by an approximate scheme that takes into account the fact that the tubes are cylinders rather than lines. In particular geometries, the carbon atoms of a tube would interact more strongly with those of the adjacent tube rather than those atoms on the opposite side of the same cylinder. Hence, in terms of modelling the tubes as one-dimensional rods in the potential calculation, the effective atomic density of the rod can be considered to be displaced towards another rod by a distance $q1$ (approximately

the radius of the tube) instead of being centred in the middle of the rod. The shifted atomic density has to be representative of the proportion of atoms primarily contributing to the potential from this part of the cylinder and so it has to be decreased in magnitude by a factor $q2$. Eq. (4) then becomes

$$(R(n, m) + q1)^2 = \Delta x(n, m)^2 + \Delta y(n, m)^2 + \Delta z(n, m)^2$$

and Eq. (3)

$$V_{\text{segment}} = -C_6Aq_2^2/R^6 + C_{12}Bq_2^2/R^{12}.$$

Our (10,10) tubes with a diameter of 1.35 nm, and values of $q1$ and $q2$ of 1.305 nm and 0.24 respectively, yielded a potential energy surface for parallel tubes with an equilibrium separation of 1.67 nm, and a potential minimum of 0.95 eV/nm, in accordance with the results of [24], whose model of two parallel infinitely long SWNTs was the closest potential comparison that could be made. Although their tube model is inherently three-dimensional, whilst ours is only quasi-three-dimensional, our potential allows for non-parallel orientations and finite size effects (see Fig. 3). A direct comparison of separation of parallel rods versus energy/tube length for both potentials (see Fig. 2) demonstrates comparable results. In this instance, our potential simplifies upon consideration of two parallel tubes with the same y and z coordinates to the form

$$\begin{aligned} V_{\text{tt}}(R_{\parallel}) &= \int_0^L \int_0^L \left[-\frac{AC_6q_2^2}{\left(\sqrt{R^2 + K_2^2(n-m)^2} - q1\right)^6} \right. \\ &\quad \left. + \frac{BC_{12}q_2^2}{\left(\sqrt{R^2 + K_2^2(n-m)^2} - q1\right)^{12}} \right] dmdn. \end{aligned} \quad (5)$$

Finally, for the tube–surface interaction V_{ts} , the second part of the potential of Eq. (1), a simple trigonometric relationship was used:

$$V_{\text{ts}} = C \sin \theta, \quad (6)$$

where C is the SWNT–graphite interaction at optimal parallel separation, calculated to be 1.61 eV/nm for a (10,10) tube and a graphite surface [43]. The optimum tube–surface interaction energy is

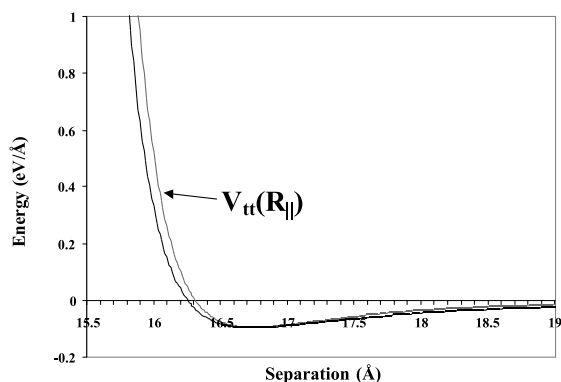


Fig. 2. Comparison between the tube–tube potential V_{tt} used in the simulations and the Girifalco et al. potential ([24]) for parallel (10,10) nanotubes. Our potential was parametrised to fit the same well depth and equilibrium separation (R_0) as the Girifalco potential using the effective separation and effective density factors q_1 and q_2 respectively. Notice the slightly shorter range of interaction. V_{tt} , unlike the potential of [24], describes also non-parallel orientations.

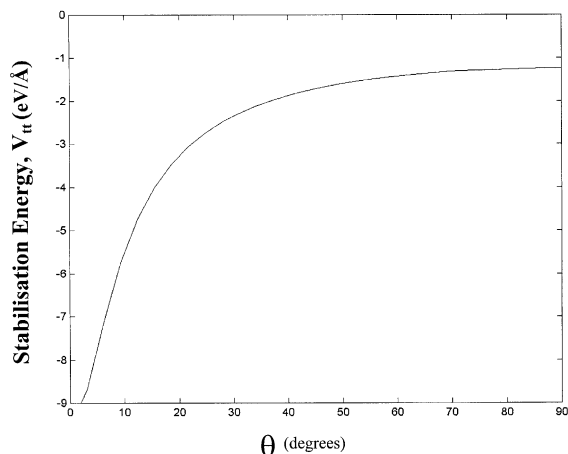


Fig. 3. Inter-tube potential V_{tt} , as a function of orientation. Here, the tubes are separated by the parallel equilibrium separation (R_0) along the x -axis. One tube remained parallel to the z -axis; the other was allowed to vary with the angle θ . The parallel configuration is considerably more stable.

therefore approximately 1.7 times larger than the tube–tube interaction energy, hence the tubes would energetically prefer settling on the surface rather than pairing up perpendicular to the surface to produce ropes.

3. Results

We applied the potential described in Section 2 to 10 nm long tubes on a graphite surface. The tubes were modelled as being 100 segments or 100 lattice units long, that is a lattice point separation of 0.1 nm was used. Initially, tubes perpendicular to the surface, were randomly distributed upon a periodic square lattice unit cell of 1000×1000 . Tubes were assumed not to interact beyond 200 lattice points in distance between x – y co-ordinates. We performed standard Metropolis Monte-Carlo simulations [44]. Random perturbations were applied to a single tube per calculation step, with perturbation parameters of: $\Delta x, \Delta y \in \{\pm 1, 0\}$, $\Delta \theta = \pm 10^\circ$, and $\Delta \phi \in \{\pm 30^\circ, 20^\circ, 10^\circ, 0^\circ\}$. However, moves that resulted in hitting tubes were rejected. On the average, simulations were run for 10^6 steps and equilibration was checked for each run. All simulations were performed at room temperature (see Fig. 4).

Our discretisation was carried out with a square lattice rather than a triangular lattice, despite nanotubes aggregating as bundles in a hexagonal fashion. What was being primarily considered with this calculation was the interaction of the tubes in the presence of a surface. Therefore, normal tube aggregation is expected to be disrupted by the conflict between the tube–tube and tube–surface interactions, depending on the relative strengths of each potential. Additionally, the small lattice point separation (13.5 lattice points per tube width) still allowed approximate hexagonal packing of the tubes. Indeed, we checked that in the absence of surface interactions, the tubes formed triangular arrangements in the simulations. Finally, because of interest in the possibility of a crossbar formation, a square lattice was considered more likely to allow such behaviour to occur, especially if the surface is chemically functionalised.

In Fig. 4 we present snapshots of the evolution of the tube structures on the surface as a function of increasing tube density. We refer to the situation of all tubes lying fully on the surface as the maximum coverage c_{\max} . We notice that the tubes arrange themselves in clusters where a few tubes orient parallel to each other as they are lying on the surface. This persists throughout. The most

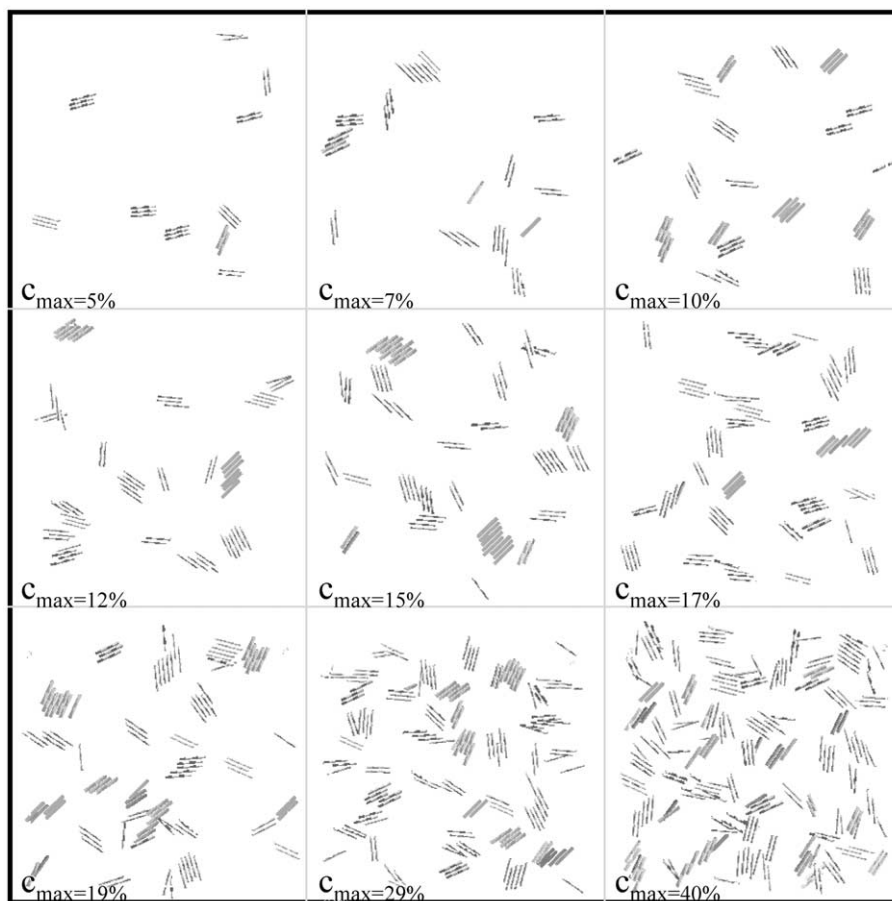


Fig. 4. Representative examples of Monte-Carlo runs of tube–surface configurations at 298 K for maximum surface coverages c_{\max} of 5–40% (top–left to bottom–right). Simulations performed in a 1001×1001 (\AA^2) periodic cell using conventional MC techniques. The actual number of tubes in each simulation is 25, 37, 50, 62, 75, 87, 100, 150, 200. Maximum coverage corresponds to all tubes lying flat on the surface. Initial increases in surface coverage led to larger two-dimensional clusters, but higher coverages demonstrate increased three-dimensional tube overlap, promoted by surface site competition.

dense system we consider, $c_{\max} = 80\%$, can be seen in Fig. 5. There are crossed tubes as often observed experimentally. These crossings would be even more frequent if the elastic energy that provides for extra stabilisation by local deformation were included [39]. The experimentally relevant region thus shows clustering and some crossing. No standing up transition is possible at these densities.

More interesting is the appearance of clusters. To quantify the cluster sizes we assigned tubes to clusters the following way: each tube was geometrically and energetically related to every other tube to determine whether the tubes were paired.

Tube pairings were determined if either of two alternative criteria, based on the definition of the tube clusters as both a geometric and an energetic phenomenon, were met. Firstly, if the tube centres were of less than a given separation, sufficiently parallel and with a minimum degree of perpendicular overlap they were considered paired. This purely geometrical routine paired those tubes suitably aligned with their immediate neighbours. Secondly, if the tube–tube interaction energy was sufficiently stabilising the tubes were paired by the calculation. Although most of the tubes satisfying the previous criterion also satisfy this one, the

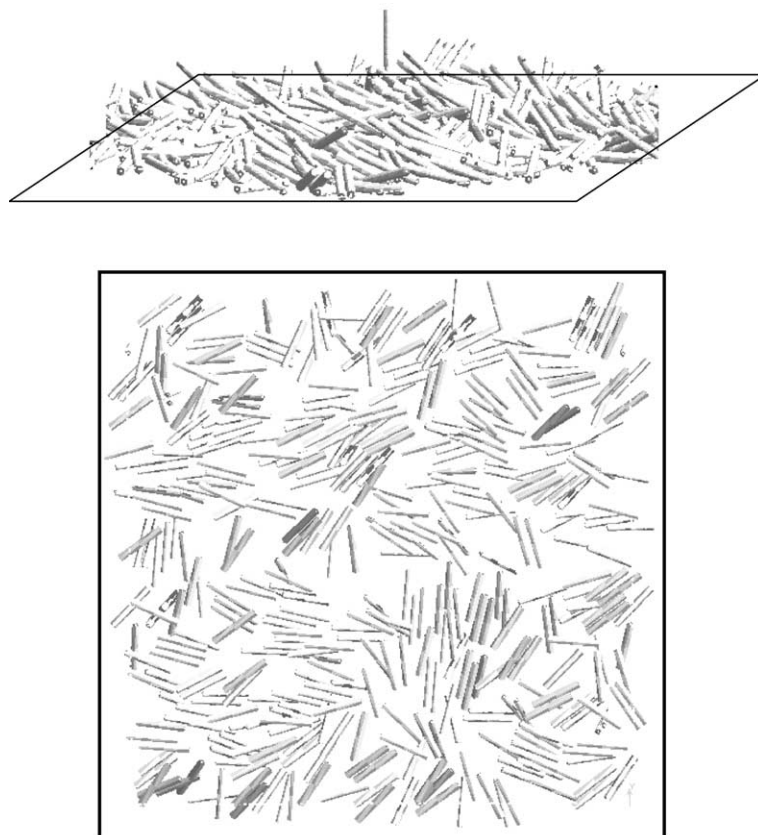


Fig. 5. Tube–surface configurations at 298 K for maximum surface coverage of 80%. Here, orderly two-dimensional clusters have become less predominant, with substantial three-dimensional cluster–cluster overlap occurring.

inclusion of this as an alternative requirement resulted in the most impartial inclusion of perpendicular tube–cluster interactions, where tubes overlapping at right angles with the direction of a cluster could be considered as part of the cluster due to their strong energetic interaction with many of the tubes constituting this cluster. The parameters used for cluster determination were chosen after iterative comparison of automated and subjective cluster analysis for numerous samples until satisfactory agreement was made (see Fig. 6).

To compare cluster sizes for different densities, it is important to normalise the results appropriately. The meaningful probability density corresponds to the fraction of tubes belonging to each cluster of a particular size. In Fig. 6 we see the results averaged over several runs for c_{\max} of 5%,

15%, 40% or 25, 75, and 200 tubes, respectively. As the density of tubes increases, bigger size clusters are observed. These densities still correspond to very dilute systems. If we instead consider the tubes all standing, then the coverage would be instead 0.5%, 1.7%, 4.5%. However, even for small densities, bigger size clusters become important and the probability of observing individual tubes decreases very rapidly.

4. Discussion

The vdW interactions of rod-like structures is an old problem, still not as well understood as those of spherical particles. In fact the geometrical anisotropy dramatically alters the phase

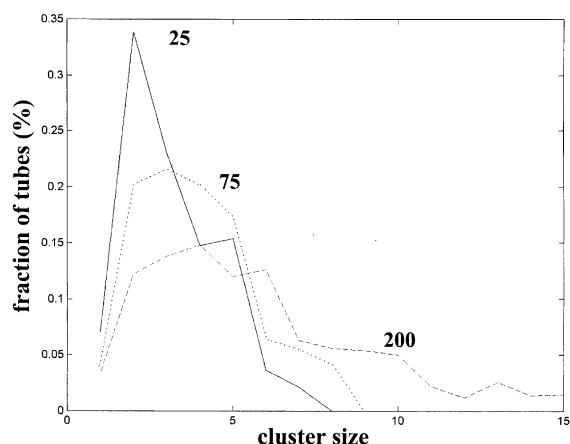


Fig. 6. Fraction of tubes in a cluster of given size for different densities. The mean number of tubes in each cluster from all runs has been normalised to the total number of tubes for each density so that a normalised probability distribution is obtained. 25 (solid line), 75 (dotted line), 200 (dashed-dotted line) tubes in a 1001×1001 (\AA^2) periodic lattice, or c_{max} of 5%, 15%, 40% are presented. The procedure for the assignment of each tube in a given cluster is described in the text. The actual parameters used for the geometric criterion are: tube centres must be less than $0.1L + 0.3L \cos \Delta\phi + 0.2 \sin \Delta \tan(\phi)$ and for the energetic: separation $< L$, and pair interaction energy > 1.37 eV.

behaviour of the system. Onsager [45] first realised this when he calculated the behaviour of very thin cylinders in the absence of attractions. The packing entropy in this case can lead to phase transitions that have been considerably studied in colloidal rods. The phase behaviour of the system becomes more complicated for strongly attracting systems. The potentials are complex and not as extensively studied. In the absence of interfaces, there is a strong driving force to align the particles [41]. The interface attraction complicates that even further. The tube–surface interaction drives the tubes on the surface until excluded volume repulsions become important. In this way it is reminiscent of monolayers that show a standing transition.

In this work we explored the molecular interactions that drive the nanotube system. We confined the study to the experimentally relevant regime and showed why tubes appear in these arrangements in current experiments. Individual tubes appear only for extremely low density sys-

tems. However, different regimes may be explored that can allow the system to order in a different fashion. In fact, nanotubes are an excellent system to test theories that consider rods as an idealised situation of more complex systems. They have very high vdW attractions, due to the special nature of carbon that allows high atomic density, and at the same they have very high aspect ratios. The magnitude of this anisotropy is unusual.

A drawback of our model is the assumption of monodispersity of single rods, clearly an idealisation as tubes of different lengths and diameters are present. The effect of polydispersity will be the subject of future work. This work can be extended in several ways: the elasticity of the tubes may be incorporated in our potentials by allowing segments to be flexible. This will allow us to study longer tubes systematically and explore the effect of geometric anisotropy. We have also ignored the solvent, that seems to play a subtle role in charging the tubes. The potentials then need to be modified to account for electrostatic interactions. A first attempt has been described in [20]. It is clear that external fields or other driving forces may keep the tubes from aggregating or impose an order. There are possibilities to control orientation through electric field induced dipoles that can align tubes with the field.

In conclusion, the unique geometrical and molecular properties of SWNTs can be used at the molecular level, a prerequisite for molecular devices, if they are prevented from forming ropes. To explore this possibility, we presented a model of low density nanotubes in the presence of an attracting surface. For experimentally relevant parameters, we observe nanotube crossings and aggregates of sizes dependent on the density. Individual tubes are improbable even for low densities.

Acknowledgements

We have greatly benefited from discussions with Jim Heath and his group. We thank Julian Gale and Ian Gould for use of their computational facilities and the E.P.S.R.C. for a quota studentship award to R.T.

References

- [1] D. Philp, J.F. Stoddard, *Angew. Chem. Int. Ed.* 35 (1996) 1155, and references therein;
D.T. Gong, T.D. Clark, J.R. Granza, M.R. Ghadiri, *Angew. Chem. Int. Ed.* 40 (2001) 988, and references therein;
G.M. Whitesides et al., *Science* 254 (1991) 1312.
- [2] See Special Issue of *Science* on Single Molecules 283 (Issue) (1999) 5408.
- [3] C. Kergueris et al., *Phys. Rev. B* 59 (1999) 1205.
- [4] R.M. Metzger, *Acc. Chem. Res.* 32 (1999) 950.
- [5] C.P. Collier et al., *Science* 289 (2000) 1172.
- [6] C. Joachim, J. Gimzewski, *Phys. Rev.* 58 (1998) 16407.
- [7] J.H. Scoen et al., *Nature* 413 (2001) 713.
- [8] J. Chen et al., *Science* 286 (1999) 1550.
- [9] A.R. Pease, *Acc. Chem. Res.* 34 (2001) 433.
- [10] V. Derycke et al., *Nano Lett.* 1 (2002) 453.
- [11] A. Bachtold, P. Hadley, T. Nakanishi, C. Dekker.
- [12] Y. Huang et al., *Science* 291 (2001) 630;
Y. Huang et al., *Science* 294 (2001) 1319.
- [13] C.A. Mirkin, M.A. Ratner, *Ann. Rev. Phys. Chem.* 43 (1992) 719;
D.L. Allara, T.D. Dunbar, P.S. Weiss, L.A. Bumm, M.T. Cygan, J.M. Tour, W.A. Reinerth, Y. Yao, M. Kozaki, L. JonesII, in: A. Aviram, M.A. Ratner (Eds.), *Molecular Electronics: Science and Technology*, Ann. N. Y. Acad. Sci., New York, 852, 1998, pp. 349–370.
- [14] S. Ijima, *Nature* 354 (1991) 56.
- [15] See for example R. Saito, G. Dresselhaus, M.S. Dresselhaus, *Physical Properties of Carbon Nanotubes*, Imperial College Press, 1998.
- [16] Y. Huang et al., *Science* 291 (2001) 630.
- [17] T. Rueckes et al., *Science* 289 (2000) 94.
- [18] S.S. Fan et al., *Science* 283 (1999) 512.
- [19] K. Yamamoto et al., *J. Phys. D* 31 (1998).
- [20] M. Diehl et al., *Angew. Chem. Int. Ed.* 41 (2002) 353.
- [21] A. Star et al., *Angew. Chem. Int. Ed.* 40 (2001) 1721.
- [22] M.L. O'Connell et al., *Chem. Phys. Lett.* 342 (2001) 265.
- [23] A. Thess et al., *Science* 273 (1996) 483.
- [24] L.A. Girifalco, M. Hodak, R.S. Lee, *Phys. Rev. B* 62 (2000) 13104.
- [25] J.R. Heath et al., *Science* 280 (1998) 391.
- [26] J. Tersoff, R.S. Ruoff, *Phys. Rev. Lett.* 73 (1994) 676.
- [27] P. Delaney et al., *Nature* 391 (1998) 466.
- [28] Y.K. Kwon, S. Saito, D. Tomanek, *Phys. Rev. B* 58 (1998) R13314.
- [29] Z.J. Donhauser et al., *Science* 292 (2001) 2303.
- [30] J.H. Scoen et al., *Science* 294 (2001) 2138.
- [31] S.N. Yaliraki et al., *J. Am. Chem. Soc.* 121 (1999) 3428.
- [32] E. Emberly, G. Kirczenow, *Phys. Rev. B* 58 (1998) 10911.
- [33] Y.G. Yoon et al., *Phys. Rev. Lett.* 86 (2001) 688.
- [34] S.N. Yaliraki, M.A. Ratner, *J. Chem. Phys.* 109 (1998) 5036.
- [35] M. Magoga, C. Joachim, *Phys. Rev. B* 59 (1999) 16011.
- [36] N.D. Lang, P. Avouris, *Phys. Rev. B* 62 (2000) 7325.
- [37] R.E. Holmlin et al., *Angew. Chem. Int. Ed.* 40 (2001) 2316.
- [38] M.S. Fuhrer et al., *Science* 288 (2000) 494.
- [39] T. Hertel, R.E. Walkup, P. Avouris, *Phys. Rev. B* 58 (1998) 13870.
- [40] J. Mahanty, B.W. Nienham, *Dispersion Forces*, Academic Press, New York, 1976.
- [41] P. van der Schoot, T. Odijk, *J. Chem. Phys.* 97 (1992) 515.
- [42] L. Girifalco, *J. Phys. Chem.* 96 (1992) 858.
- [43] A. Buldum, J.P. Lu, *Phys. Rev. Lett.* 83 (1999) 5050.
- [44] N. Metropolis, A.W. Ronenbluth, M.N. Rosenbluth, A.H. Teller, E. Teller, *J. Chem. Phys.* 21 (1953) 1087.
- [45] L. Onsager, *Ann. N. Y. Acad. Sci.* 51 (1949) 627.